Tribological behaviour at high temperature of hard CrAlN coatings doped with Y or Zr

J.C. Sánchez-López[a], A. Contreras[a], S. Domínguez-Meister[a], A. García-Luis[b], M. Brizuela[b]

[a]Instituto de Ciencia de Materiales de Sevilla (CSIC-Univ. Sevilla), Avda. Américo Vespucio 49, 41092-Sevilla, Spain

[b]TECNALIA, Mikeletegui Pasealekua, 2

20009 Donostia-San Sebastián, Spain

The tribological properties of CrAlN, CrAlYN and CrAlZrN coatings deposited by direct current reactive magnetron sputtering are studied by means of pin-on-disk experiments at room temperature, 300, 500 and 650 ºC using alumina balls as counterparts. The influence of the metallic composition (Al, Y and Zr) on the friction, wear properties and oxidation resistance is studied by means of scanning electron microscopy, energy dispersive X-ray analysis and Raman analysis of the contact region after the friction tests. The results obtained allow us to classify the tribological behaviour of the CrAl(Y,Zr)N coatings into three groups according to the nature of the dopant and aluminium content. The sliding wear mechanism is characterized by the formation of an overcoat rich in chromium and aluminium oxides whose particular composition is determined by the initial chemical characteristics of the coating and the testing temperature. The fraction of Cr_2O_3 becomes more significant as the Al content decreases and the temperature increases. The addition of Y, and particularly Zr, favours the preferential formation of Cr_2O_3 versus CrO_2 leading to a reduction of friction and wear of the counterpart. Conversely, the tribological behaviour of pure

CrAlN coatings is characterized by higher friction but lower film wear rates as a result of higher hardness and major presence of aluminium oxides on the coating surface.

Keywords: CrAlN, yttrium, magnetron sputtering, friction, oxidation, wear, tribolayer, Raman

1. Introduction

Recently, CrAlN films grown by physical vapour deposition have gained much attention as a promising substitute for TiAlN coatings. This is mainly possible due to their superior hot hardness and oxidation resistance [1,2]. CrAlN have proven to be effective protective coatings for machining applications of hard-to-cut materials where elevated stress and temperature appear on the cutting tool surface or when dry operations are demanded [3-8]. The incorporation of Al to CrN promotes higher hardness, thermal and chemical stability, allowing increased efficiency of cutting and forming tools [9-11]. The relative concentration of Al inside the coating, Al/(Al+Cr), is tried to be fixed below 0.7 in order to form the metastable solid solution of Al inside the face-centered cubic (fcc) CrN lattice [12,13]. The formation of hexagonal compact packing (hcp) AlN structure brings about lower hardness and elastic moduli, which results in lower wear resistance. When exposed to air at elevated temperatures, CrAlN films form dense and adherent mixed aluminium and chromium oxide scales [3,9,14], which eventually suppress the oxygen diffusion into the bulk, providing excellent oxidation resistance up to temperatures as high as 900ºC [1,15-17]. Current investigations seek to improve the thermal and oxidation resistance above this limit temperature by incorporation of large (substitutional) atoms, as they effectively retard diffusion related processes (recovery, decomposition and recrystallization). Ytrium has been proposed to improve oxidation resistance beyond 1100ºC by segregation to the oxide scale grain boundaries, blocking fast diffusion paths [11,15,18-20]. Moreover, the addition of a reactive element was suggested to reduce the accumulation of voids at the substrate/scale interface [21]; to improve the mechanical properties of the scale by modifying its structure [22] or to prevent the grain coarsening at elevated temperatures [23]. In a previous work we also confirmed the improved oxidation resistance of a

CrAlYN coating in comparison to CrAlZrN [24]. The tribological properties of CrAlN coatings have been investigated previously [6,7,25-27] but only limited information is available about their tribological behavior at high temperature [28-30]. Other studies have explored the enhancement of tribological properties by alloying carbon or vanadium that promote the formation of lubricant tribo-layers [31,32]. The present work was undertaken to have an overview on the tribological behaviour of these coatings at elevated temperature, to determine the processes governing the friction and wear behaviour, and finally, to assess the influence of the dopant nature and chemical composition on the observed tribological performance.

2. Experimental

CrAl(Y,Zr)N coatings were prepared on M2 steel substrates by direct current magnetron sputtering using Ar/N_2 mixtures in a commercial equipment (CemeCon® CC800/8) provided with four rectangular targets (200 mm × 88 mm × 5 mm). The used target materials were chromium (99.9% purity), aluminium (99.5% purity), alloyed Al/Cr-10%, alloyed Al/Cr-20%, yttrium (99.5% purity) or zirconium (99.5% purity). The base pressure of the vacuum chamber was $\sim 1\times10^{-4}$ Pa and the deposition pressure set at 1 Pa, with an Ar/N_2 ratio of 1.5. The Al concentration was tuned inside the coatings by increasing the numbers of Al targets, using mixed Al/Cr alloys and appropriate selection of the sputtering power from 1000 to 3000W. The dopant content was changed by including one target of Y or Zr at a power of 1500 W or 3000 W. The sputtering conditions were set at 3000 W for chromium target in all cases. The sample holder was negatively biased in the range from 110 to 120 V and the temperature ranged from 200 to 400 °C. The film thickness values typically fall in the 2–4 μm range.

Chemical composition of the samples was obtained by electron probe microanalysis (EPMA). The EPMA equipment was a JEOL JXA-8200 SuperProbe instrument equipped with four wavelengths detectors (WDS) and one energy-dispersive X-ray (EDX) detector. Examination of the wear scars was done by scanning electron microscopy (SEM) performed in a high resolution FEG microscope, HITACHI-4800 coupled with an EDX detector. Raman spectroscopy spectra measurements (150-1200 cm^{-1}) were carried out with a LabRAM Horiba Jobin Yvon spectrometer equipped with a CCD detector and a He-Ne laser (532 nm) at 5 mW. All the samples were analysed during 100 s of exposure time and an aperture hole of 100 μm. The mechanical properties were measured with a Fischerscope H100 dynamic microprobe instrument using a Vickers indenter and a load range from 0.4 to 10 mN in 40 load steps, with resolution better than 0.02 mN. The time between two load steps was 0.5 s and the test cycle was loading and unloading. Measurement of the indentation depth was achieved with a capacitance displacement gauge of 2 nm-accuracy. Ten measurements were done in different locations for each sample. The maximum load was selected in such a way that the maximum indentation depth did not exceed 10–15% of the coating thickness in order to avoid the influence of the substrate. The area correction factor to account for tip blunting was estimated using a silicon wafer as reference. An indentation size effect correction factor was applied by the Fischercope software using the same material to correct the increase of hardness with decreasing depth of penetration although some hardness overestimation is still likely at very small indentations. The hardness and reduced Young's modulus were calculated from the load–unload displacement curves using the Oliver and Pharr method.

The tribological properties of the coatings were evaluated by ball-on-disk friction tests in a Microtest high-temperature tribometer in rotative motion in ambient air (RH:

30-40%) at room temperature and heating at 300, 500 and 650 ºC. The test parameters were set to 5 N of applied load (maximum initial Hertzian contact pressure of 1.45 GPa) and 10 cm/s of linear speed using alumina balls as counterparts. The number of cycles was 20000 for the room temperature tests and 2500 for the rest. At least two tests were performed for each type of coating. Normalized wear rates (mm^3/Nm) were evaluated from cross-sectional profiles taken across the disk-wear track by means of stylus profilometry.

3. Results and discussion

3.1. Film chemical composition

Table 1 reports the chemical composition of the CrAl(Y,Zr)N under study as measured by EPMA. The Al content varies between 3 and 31 at.% while the dopants (Y or Zr) are restricted below 4 at.%. It has been found that excessive yttrium incorporation (>4 at.%) results to be detrimental for the oxidation resistance [18]. The first set of coatings is composed of three CrAlN films (CrAlN-1, CrAlN-2, CrAlN-3) with growing Al content and without dopant. The Al/(Al+Cr) ratios change from 0.09 to 0.68, close to the limit of the hexagonal wurzite transformation. The influence of the dopant (Y or Zr) at similar Al incorporation is determined from the next pair of samples formed by CrAlZrN and CrAlYN-1 films. The last couple is a set of two CrAlYN samples (CrAlYN-2 and CrAlYN-3) with similar Y dopant content but different Al/(Al+Cr) ratios (0.09 and 0.48), from the low and high Al content regime respectively.

3.2. Tribological results

a) Influence of the Al content

Fig. 1 shows the friction coefficient and film wear rates measured for the CrAlN-1, CrAlN-2, CrAlN-3 coatings with increasing Al contents (8, 21 and 31 at.%) or (0.19, 0.50 and 0.68 if expressed in terms of Al/(Al+Cr) ratio) at the four testing temperatures (ambient, 300, 500 and 650ºC). The friction coefficient values remain high (0.5-0.9), as expected for hard transition metal nitrides in unlubricated sliding tests [26-30], although a trend to decrease is observed for temperatures above 300ºC. A maximum friction coefficient was previously observed at 200ºC in TiAlCN films and attributed to the removal of condensed water vapour film from the sliding surface which has a lubricious effect [31]. Comparatively, the CrAlN-3 sample with the highest Al content is the one showing the highest friction values, between 0.7 and 0.9. In general for all coatings, although the film resistance is improved for higher Al content, the wear rates exhibit an increment as the temperature rises. Particularly, the CrAlN-3 sample showed no measurable wear for tests carried out below 650ºC.

b) Influence of the dopant

Fig. 2 plots the tribological behaviour of the doped samples at two different Al/(Al+Cr) rates (<0.1 and ≈0.5) which will help us to check the influence of the dopant concentration and chemical nature. Comparing CrAlYN-1 and CrAlYN-2, we can infer the influence of Y concentration (1.6 and 3.9 at.%) at Al/(Al+Cr) < 0.1 on the tribological properties. The friction coefficient and wear rate present similar patterns and no clear differences can be noticed. Both coatings show a maximum friction coefficient at 300ºC of about 0.8 that decreases continuously as the temperature of the test increases. In the case of the Zr-doped sample the friction coefficient exhibits a similar trend although the drop after 300ºC is more noticeable, reaching average values below 0.5 at 650ºC. This diminution of the friction coefficient goes along with a

decrease of the wear rates showing improved performance than CrAlYN samples. Finally, the last sample with Al/(Al+Cr) = 0.5 and yttrium content of 1.6 at.% exhibits higher mean friction coefficients (between 0.6 and 0.8) and lower wear rates. This conclusion is in agreement with the previous results obtained with the pure CrAlN films. Summarizing, at low Al content Zr incorporation provides better tribological performance but combining yttrium with higher Al content the results are improved.

To illustrate better the benefits of the dopant element, Fig. 3 shows the comparison of the results obtained with the doped samples CrAlZrN (2 at.% Zr) and CrAlYN-3 (1.6 at.% of Y) with their respective undoped samples CrAlN-1 and CrAlN-2 with similar Al/(Al+Cr) ratios. It is clearly inferred that Zr-doped samples improves the behaviour of the corresponding CrAlN-1 samples at any temperature whilst the Y favours the wear resistance up to 500ºC but has almost no effect at 650ºC. The friction curves for these samples at 650ºC are shown in Fig. 4 together with the optical micrographs taken for both counterfaces (ball and track). The most striking difference is the higher mean values and dispersion obtained with the samples of the right column, belonging to the highest Al content and the steady-state reached with the Zr sample. According to the optical micrographs, the CrAlN-1 is the one showing the highest amount of debris on the ball counterface and eroded wear track as corresponds to the highest wear rate obtained for this film. On the contrary, the wear track in the Zr sample appears filled with smeared material.

A final look was carried out on the ball wear rates for all films. The highest worn volumes correspond to the tests giving the highest friction coefficients (particularly at 300ºC) shown by the hardest samples (CrAlZrN [33 GPa], CrAlYN-3 [30 GPa] and CrAlN-3 [40 GPa]). These results are in agreement with a major abrasive wear in these conditions. It is worth mentioning that tribological behaviour is highly dependent on the

nature of the counterface material and different trends to that noted here can be found [29]. For instance, by using ductile materials as Ti or Al alloys, the adhesion of material from the counterpiece is increased and the coefficient of friction is predominately defined by the shear properties of this transfer layer and the ball.

c) Post-test analysis of the wear tracks

In order to understand the wear mechanism and the physic-chemical transformation induced during the oxidative friction conditions, a careful examination of the wear tracks was done for the best doped samples (CrAlZrN and CrAlYN-3) compared to a representative good CrAlN sample (CrAlN-2) at the maximum testing temperature of 650ºC. Fig. 6 shows the SEM pictures, oxygen distribution and EDX spectra associated to the three wear tracks. The images of the wear track denote higher presence of debris particles accumulated along the borders for the undoped and Y-doped samples while the Zr-sample appears filled with material, as observed in the optical micrographs. Likewise, the aspect of the first track corresponding to the pure CrAlN agrees with a typical abrasive wear with deep groves inside the track while the track on CrAlZrN can match better with an adhesive wear. In the case of CrAlYN tracks, marked grooves and adhered material in the form of bands are observed inside the track. When the oxygen elemental mapping is measured for these tracks it is observed that the distribution is rather homogeneous in the case of CrAlZrN, while in the others oxygen appeared concentrated at the borders and adhered material. These results point to the formation of a tribolayer in the CrAlZrN while the wear of CrAlN and CrAlYN coatings is mainly abrasive with ejection of the debris particles along the sides of the track. Previous oxidation studies performed on these coatings up to 1000ºC in air demonstrated the formation of a thicker oxide scale in the case of CrAlZrN coatings and Zr was not

diffusing to the surface together with Cr and Al [24]. The steady and smooth friction curve observed for this CrAlZrN coating at 650ºC indicates a good adhesion of this tribo-oxide layer, since the detachment of a large volume of material in the wear track would generate an abrupt friction change.

Fig. 6 also includes the EDX spectra taken in the centre and borders of the wear track for each system. Oxygen peak is detected in all the samples together with the metallic elements, particularly at the track edges when oxide debris accumulates. In agreement with previous works [24, 33], this is indicative of the formation of aluminium and chromium oxides as a consequence of tribo-oxidation in the contact. Except in the CrAlZrN, the relative Cr/Al proportion is almost the same at the centre and border position. The observed Cr enrichment in the wear track is indicating a preferential formation of chromium oxides for this sample as will be further demonstrated by Raman analysis.

Raman spectroscopy has proven to be a powerful tool to study worn surfaces and define the phase composition of the wear products enabling the elucidation of the friction mechanisms [34-36]. Fig. 7 depicts the Raman spectra taken from the wear tracks obtained at room temperature, 300ºC and 650ºC for all the coatings ordered by increasing Al/(Al+Cr) ratio. The intermediate point at 300ºC was selected as this temperature usually exhibits the maximum friction coefficient and ball wear volumes.

At room temperature, the Raman spectrum of the coating with the lowest Al content (CrAlYN-1) shows the peaks of Cr_2O_3 at 307, 545 cm^{-1}, CrO_2 at 688 cm^{-1} and a small band at ~870 cm^{-1} that can be attributed to Cr_2O_5 and/or Cr_8O_{21} phases [37,38,39]. Eventually, the presence of CrO_3 is determined by the presence of a peak situated at around 1005 cm^{-1} [37,40]. As the aluminium content increases, the relative proportion of chromium oxides decreases and the development of a broad band at about 250 cm^{-1}

related with the acoustic mode of cubic Cr(Al)N phase [38] becomes more evident. Thus, for the sample CrAlN-3 with the highest Al content, the main peak is located at 760 cm^{-1}, more in agreement with Al_2O_3 predominance [41].

At 300ºC, the formation of Cr_2O_3 is hardly detected being a mixture of CrO_2 and Al_2O_3 the predominant peaks along the series. Other found peaks correspond to Cr_2O_5 at ~880 cm^{-1} and CrO_3 at 1010 cm^{-1} for the CrAlZrN sample.

In the last column, the spectra taken at 650ºC denote that the intensity of the peak at 545 cm^{-1} is higher for coatings with Al/(Al+Cr)<0.5. This typical band of Cr_2O_3, the most thermodynamically stable chromium oxide, indicates the major presence of this type of chromium oxide. From this point the main peak is found at about 700 cm^{-1} and shifts gradually towards higher values as the aluminium content increases. This can be explained by a gradual enrichment of Al_2O_3 with respect to chromium oxides (CrO_2 and Cr_2O_3) in the composition of the wear products. This behaviour is general for all the temperatures and correlates with an increment of the friction coefficient observed for samples with higher Al content. On the other side, the friction coefficient drops as the temperature rises and the Al/(Al+Cr) is lower since it favours the formation of Cr_2O_3 versus hard alumina. A summary of oxide products determined by Raman analysis for the studied samples is displayed in Table 2.

This Raman study has allowed us to conclude that the wear material is formed mainly by a mixture of chromium oxides with different stoichiometries and alumina. The predominance of the Cr_2O_3 is associated with lower friction coefficients as observed in samples tested at 650ºC. Nevertheless, at 300ºC the major phases are found to be other chromium oxide phases (CrO_2, Cr_2O_5, CrO_3) which are responsible of the high friction coefficients measured at this particular temperature.

3.3. Schematic frictional model: final discussion

As a result of the current investigations we can propose a model to explain the CrAl(Y,Zr)N tribological behaviour as a function of the aluminium content and dopant presence at high temperature (cf. Fig. 8). The steady-state found in the case of CrAlZrN is thus associated to the formation of a third-body layer composed mainly of Cr_2O_3 that replenishes the contact preserving low shear conditions. The second group is formed by Y-doped samples and pure CrAlN samples with Al/(Al+Cr) ratios between 0.2 and 0.5. In this case, a mixture of Cr_2O_3 and Al_2O_3 and an abrasive wear mechanism were identified; concerning the tribological properties, the film wear resistance is improved but average friction coefficients are also higher. The last type of wear corresponds to CrAlN with very high aluminium content (Al/(Al+Cr)>0.6) but still below the cubic-hexagonal transition. In this case, the tribological behaviour is characterized by a severe polishing of the ball counterface but at a low film wear rate. In these conditions, the film hardness and friction coefficient attain their maximum values. This conclusion is in agreement with previous works showing that at elevated temperatures the fcc-CrAlN films with maximum aluminium content outperform the coatings with lower Al-content [4,29]. It is also possible, as suggested in previous works, that at these Al content, some aluminium atoms segregate along the grain boundaries to form amorphous AlN phase that contributes to hardness increment by blocking grain boundary sliding during deformation [42]. The achievement of higher hardness in CrAlN-3 ($Cr_{0.32}Al_{0.68}N$) could be indicative of an strengthening effect by reduced grain size and mobility. The outstanding tribological performance can be attributed to excellent oxidation resistance in CrAlYN-3 and CrAlN-3 combined with hot hardness [4].

In summary, the Zr-doped would be of interest for tribological hot applications where lower and stable friction is requested while hard cubic CrAlN with high Al

contents would be the most advantageous for withstanding high temperatures. Certain incorporation of yttrium can help to form protective tribofilms and preserve the grain coarsening at elevated temperatures. Nevertheless, we should keep in mind that industrial operations involve more material transfer between coating and counterface than on pin-on-disc tests and, therefore, industrial trials should be carried out in each specific case for validation.

4. Conclusions

The sliding tribological behaviour of doped CrAlN films with Y or Zr and variable Al content are comparatively studied with pure undoped CrAlN films at temperatures from ambient to 650ºC using alumina balls as counterpart. A general increase of the film wear rate is observed with the temperature. The friction coefficient reaches a maximum at 300ºC and then diminishes as the film oxidation proceeds. The main wear products were chromium oxides with different stoichiometries and alumina. The fraction of Cr_2O_3 becomes more significant as the Al content decreases and the temperature increases. This chemical transformation leads to a decrease of the friction coefficient at expenses of a reduction of the film wear resistance.

The incorporation of dopants in $Cr_{1-x}Al_xN$ films can be beneficial if aluminium contents are not close to the maximum possible in metastable cubic solution [$x \approx 0.6$-0.7]. The CrAlZrN layer is less oxidation resistant, promoting the formation of a Cr_2O_3 – rich tribolayer that decreases friction and wear. The addition of Y (up to 2 at.%) helps to reduce the film wear up to 500ºC but becomes comparable to undoped CrAlN with similar Al content at 650ºC. For high Al content in cubic structure ($Cr_{0.32}Al_{0.68}N$), high hardness and outstanding film wear resistance can be obtained. However, high abrasion

of ball counterface and higher friction coefficients are obtained in comparison with the yttrium-doped ones.

Acknowledgements

The Spanish MINECO (projects Nº MAT2011-29074-C02-01/-02 and CONSOLIDER FUNCOAT CSD2008-00023) is acknowledged for financial support.

References

1. M. Kawate, A.K. Hashimoto, T. Suzuki, Surf. Coat. Technol. 165 (2003)163.

2. Y.C. Chim, X.Z. Ding, X.T. Zeng, S. Zhang, Thin Solid Films 517 (2009) 4845.

3. O. Banakh, P. E. Schmid, R. Sanjinés, F. Lévy, Surf. Coat. Technol. 163–164 (2003) 57.

4. A.E. Reiter, V.H. Derflinger, B. Hanselmann, T. Bachmann, B. Sartory, Surf. Coat. Technol. 7 (2005) 2114.

5. J.C. Sánchez-López, D. Martínez-Martínez, C. López-Cartes, A. Fernández, M. Brizuela, A. García-Luis, J.I. Oñate, J. Vac. Sci. Technol. A 23, 681-686 (2005).

6. M. Brizuela, A. García, I. Braceras, J.I. Oñate, J.C. Sánchez-López, D. Martínez-Martínez, C. López-Cartes, A. Fernández, Surf. Coat. Technol. 200, 192-197 (2005).

7. J. Lin, B. Mishra, J.J. Moore, W.D. Sproul, Surf. Coat. Technol. 201 (2006) 4329.

8. H.C. Barshilia, N. Selvakumar, B. Deepthi, K.S. Rajam, Surf. Coat. Technol. 201 (2006) 2193.

9. J.L. Endrino, G.S. Fox-Rabinovich, A. Reiter, S.V. Veldhuis, R. Escobar Galindo, J.M. Albella, J.F. Marco, Surf. Coat. Technol. 201 (2007) 4505.

10. L. Wang, X. Nie, J. Housden, E. Spain, J.C. Jiang, E.I. Meletis, A. Leyland, A. Matthews, Surf. Coat. Technol. 203 (2008) 816.

11. K.-D. Bouzakis, N. Michailidis, S. Gerardis, G. Katirtzoglou, E. Lili, M. Pappa, M. Brizuela, A. Garcia-Luis, R. Cremer, Surf. Coat. Technol. 203 (2008) 781.

12. H. Hasegawa, M. Kawate, T. Suzuki, Surf. Coat. Technol. 200 (2005) 2409.

13. P.H. Mayrhofer, D. Music, Th. Reeswimkel, H.-G. Fuss, J.M. Schneider, Acta Mater. 56 (2008) 2469.

14. R. Escobar Galindo, J.L. Endrino, R. Martínez, J.M. Albella, Spectrochimica Acta Part B 65 (2010) 950–958.

15. R. Braun, F. Rovere, P.H. Mayrhofer, C. Leyens, Intermetallics 18 (2010) 479.

16. H. Willmann, P.H. Mayrhofer, P.O.A. Persson, A. E. Reiter, L. Hultman, C. Mitterer, Scripta Mater. 54 (2006) 1847.

17. H.C. Barshilia, B. Deepthi, K.S. Rajam, K.P. Bhatti, S. Chaudhary, J. Vac. Sci. Technol. A 27 (2009) 29.

18. F. Rovere, P. H. Mayrhofer, A. Reinholdt, J. Mayer, J.M. Schneider, Surf. Coat. Technol. 202 (2008) 5870.

19. F. Rovere, P. H. Mayrhofer, J. Vac. Sci. Technol. A 26 (2008) 29.

20. F. Rovere, D. Music, J. M. Schneider, P. H. Mayrhofer, Acta Mater. 58 (2010) 2708.

21. D.P. Whittle, J. Stringer, Philos. Trans. R. Soc. London Ser. A-Math. Phys. Eng. Sci. 295 (1980) 309.

22. Y. Saito, T. Maruyama, T. Amano, Mater. Sci. Eng. 87 (1987) 275.

23. Harish C. Barshilia, Shashidhara Acharya, Moumita Ghosh, T. N. Suresh, K.S. Rajam, Manohar S. Konchady, Devdas M. Pai, Jagannathan Sankar, Vacuum 85 (2010) 411.

24. T.C. Rojas, S. El Mrabet, S. Domínguez-Meister, M. Brizuela, A. García-Luis, J.C. Sánchez-López, Surf. Coat. Technol. 211 (2012) 104-110.

25. Xing-Zhao Ding, X. T. Zeng, Surf. Coat. Technol. 200 (2005) 1372.

26. J.L. Mo, M. H. Zhu, B. Lei, Y.X. Leng, N. Huang, Wear 263 (2007) 1423.

27. J.E. Sánchez, O.M. Sánchez, L. Ipaz, W. Aperador, J.C. Caicedo, C. Amaya, M.A. Hernández Landaverde, F. Espinoza Beltrán, J. Muñoz-Saldaña, G. Zambrano, Appl. Surf. Sci. 256 (2010) 2380.

28. S. R. Pulugurtha, D. G. Bhat, M. H. Gordon, J. Shultz, M. Staia, S. V. Joshi, S. Govindarajan, Surf. Coat. Technol. 202 (2007) 1160.

29. A. E. Reiter, C. Mitterer, M. Rebelo de Figueredo, R, Franz, Tribol. Lett. 37 (2010) 605.

30. Tomas Polcar, Tomas Vitu, Jozef Sondor, Albano Cavaleiro, Plasma Process. Polym. 6 (2009) S935.

31. G. Kamath, A. P. Ehiasarian, Y. Purandare, P. Eh. Hovsepian, Surf. Coat. Technol. 205 (2011) 2823.

32. R. Franz, J. Neidhart, R. Kaindl, B. Sartory, R. Tessadri, M. Lechthaler, P. Polcik, C. Mitterer, Surf. Coat. Technol. 203 (2009) 1101.

33. T. Polcar, R. Martinez, T. Vitu, L. Kopecky, R. Rodriguez, A. Cavaleiro, Surf. Coat. Technol. 203 (2009) 3254.

34. J.C. Sánchez-López, D. Martínez-Martínez, C. López-Cartes, A. Fernández, Surf. Coat. Technol. 202, 4011-4018 (2008).

35. J.C. Sánchez-López, D. Martínez-Martínez, M.D. Abad, A. Fernández. Surf. Coat. Technol. 204, 947-954 (2009)

36. S. El Mrabet, M.D. Abad, J.C. Sánchez-López, Surf. Coat. Technol. 206, 1913-1920 (2011).

37. O. Monnereau, L. Tortet, C.E.A. Grigorescu, D. Savastru, C. R. Iordanescu, F. Guinneton, R. Notonier, A. Tonetto, T. Zhang, I.N. Mihailescu, D. Stanoi, H.J. Trodahl, J. Opto. Adv. Mater. 12 (2010) 1752.

38. H.C. Barshilia, K.S. Rajam, J. Mater. Res. 19 (2004) 3196.

39. A. Ozturk, K.V. Ezirmik, K. Kazmanli, M. Urgen, O.L. Erylmaz, A. Erdemir, Tribol. Int. 41 (2008) 49.

40. Sonoko Kikuchi, Katuteru Kawauchi, Masaru Kurosawa, Hisashi Honjho, Teruo Yagishita, Anal. Sci. 21 (2005) 197.

41. A. Misra, H. D. Bist, M. S. Navati, R.K. Thareja, J. Narayan, Mater. Sci. Eng. B 79 (2001) 49.

42. Zhao Li, Paul Munroe, Zhong-tao Jiang, Xiaoli Zhao, Jiang Xu, Zhi-feng Zhou, Jian-qing Jiang, Feng Fang, Zong-han Xie, Acta Mater. 60 (2012) 5735.

Figure captions

Fig. 1. Dependence of the tribological properties (friction coefficient and wear rate) for CrAlN films with different Al contents.

Fig.2. Dependence of the tribological properties (friction coefficient and wear rate) for CrAlZrN and CrAlYN films.

Fig. 3. Comparative analysis of the tribological properties (friction coefficient and wear rate) of Zr or Y-doped CrAlN coatings vs. CrAlN of similar Al contents.

Fig. 4. Friction curves at 650ºC of Zr or Y-doped CrAlN coatings vs. CrAlN of similar Al contents. The optical pictures taken from the ball scar and wear tracks are shown as insets.

Fig.5. Ball wear rates and friction coefficients measured for all the CrAl(Y,Zr)N coatings under study.

Fig. 6. SEM pictures, oxygen mapping and EDX spectra associated to the wear tracks obtained at 650ºC for the tree types of coatings: CrAlN (CrAlN-2), CrAlZrN and CrAlYN (CrAlYN-3).

Fig. 7. Raman spectra taken from the wear tracks obtained at room temperature, 300ºC and 650ºC for all the coatings ordered by increasing Al/(Al+Cr) ratios.

Fig. 8. Scheme illustrating the three types of wear mechanism identified in this work depending on the aluminium content and nature of the dopant element.

Tables

Table 1. Chemical composition, thickness and mechanical properties of the CrAlN, CrAlZrN and CrAlYN coatings.

Sample	Al / (Cr+Al)	Cr	Al	Y or Zr	N	thickness	H	E
		at. %				(µm)	(GPa)	(GPa)
CrAlN-1	0.19	36.5	8.3	0	55.2	3.3	30	304
CrAlN-2	0.50	20.5	20.5	0.0	55.0	2.6	28	210
CrAlN-3	0.68	14.5	30.8	0.0	54.7	2.1	40	274
CrAlZrN	0.10	38.8	4.5	2	54.8	2.8	33	317
CrAlYN-1	0.06	39.7	2.6	3.9	53.8	4.0	30	217
CrAlYN-2	0.09	40.1	4	1.6	54.3	3.8	24	187
CrAlYN-3	0.48	24.1	22.0	1.6	53.9	3.3	29	217

Table 2. Summary of the Raman analysis of the wear track after testing at 650ºC.

Main Phase	Other phases	Samples	Al / (Al+Cr)
Cr_2O_3	CrO_2 Cr_2O_5 Al_2O_3 CrO_3	CrAlYN-1 CrAlYN-2 CrAlZrN	0.06 0.09 0.10
Cr_2O_3+Al_2O_3		CrAlN-1	0.19
Al_2O_3	Cr(Al)N	CrAlYN-3 CrAlN-2 CrAlN-3	0.48 0.50 0.68

Figure 1

Click here to download high resolution image

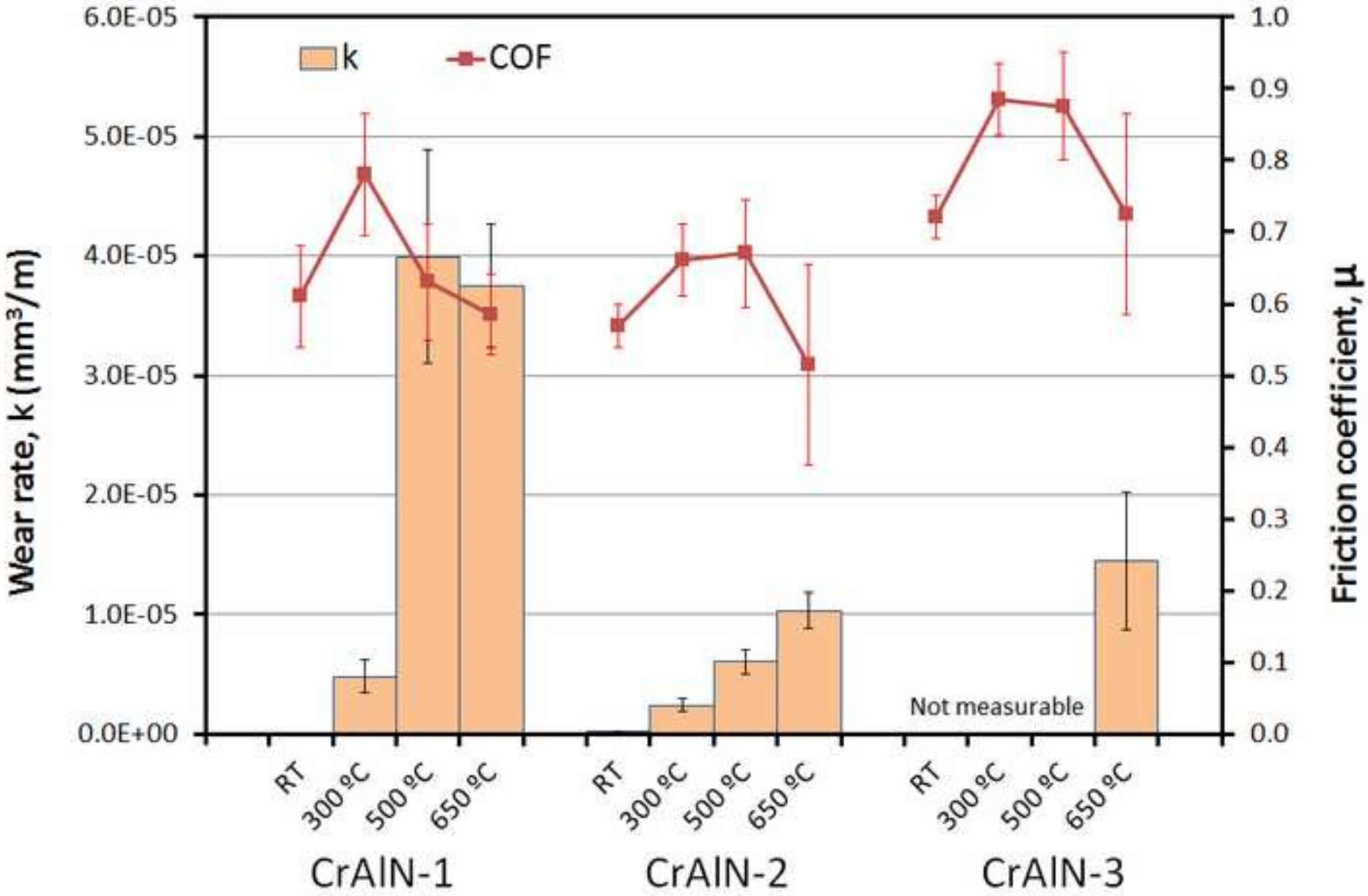

Figure 2

Click here to download high resolution image

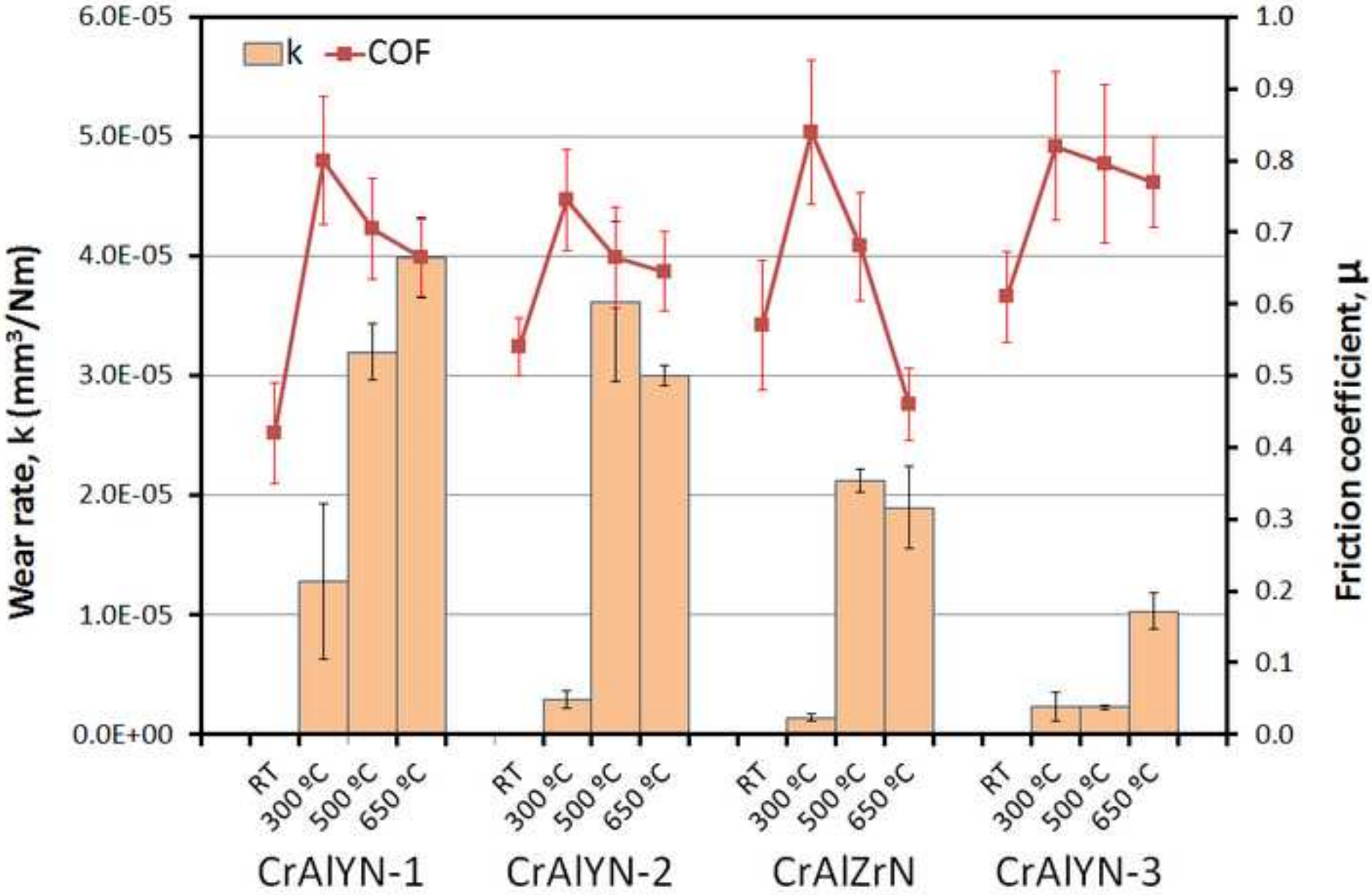

Figure 3

Click here to download high resolution image

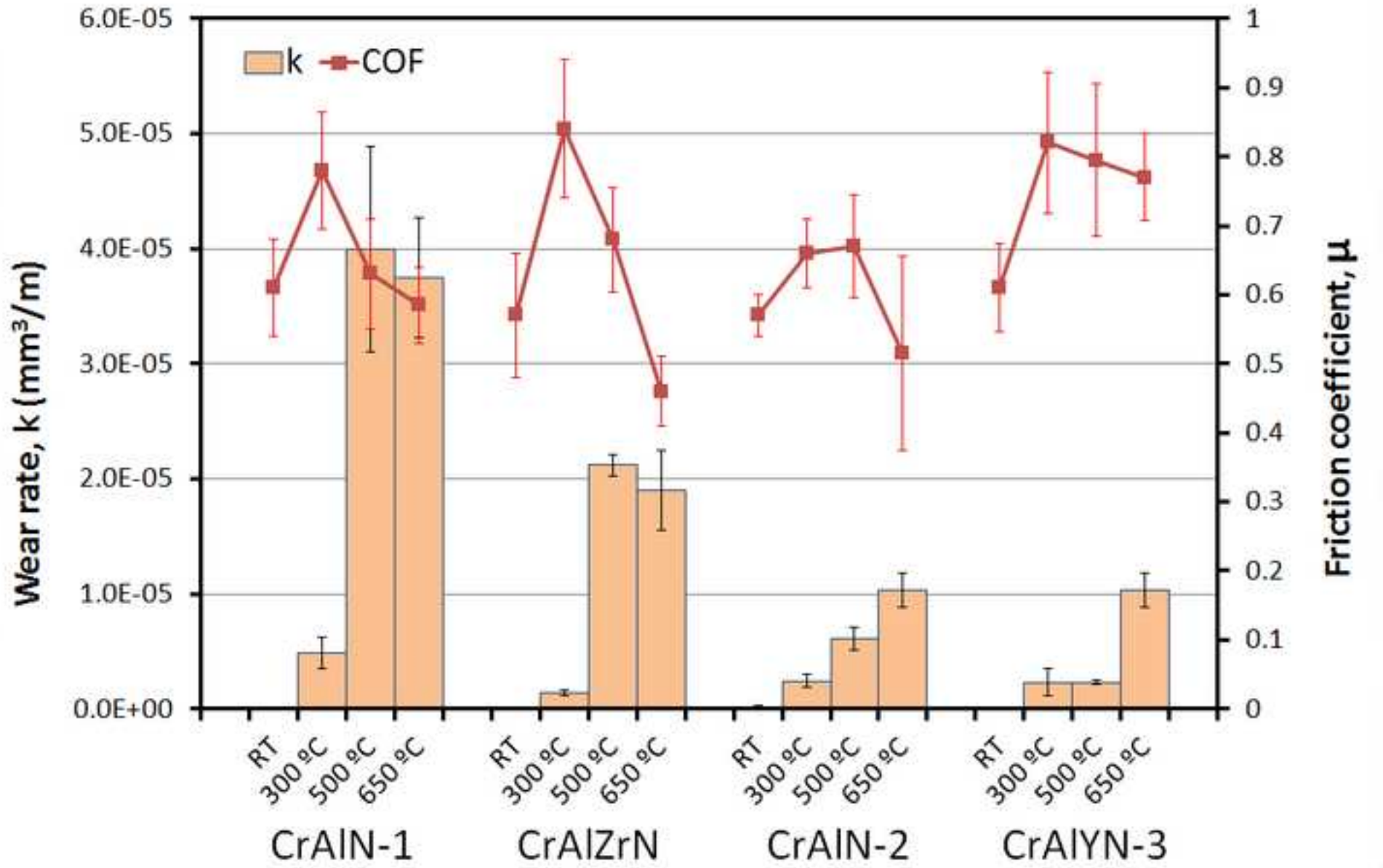

Figure 4

Click here to download high resolution image

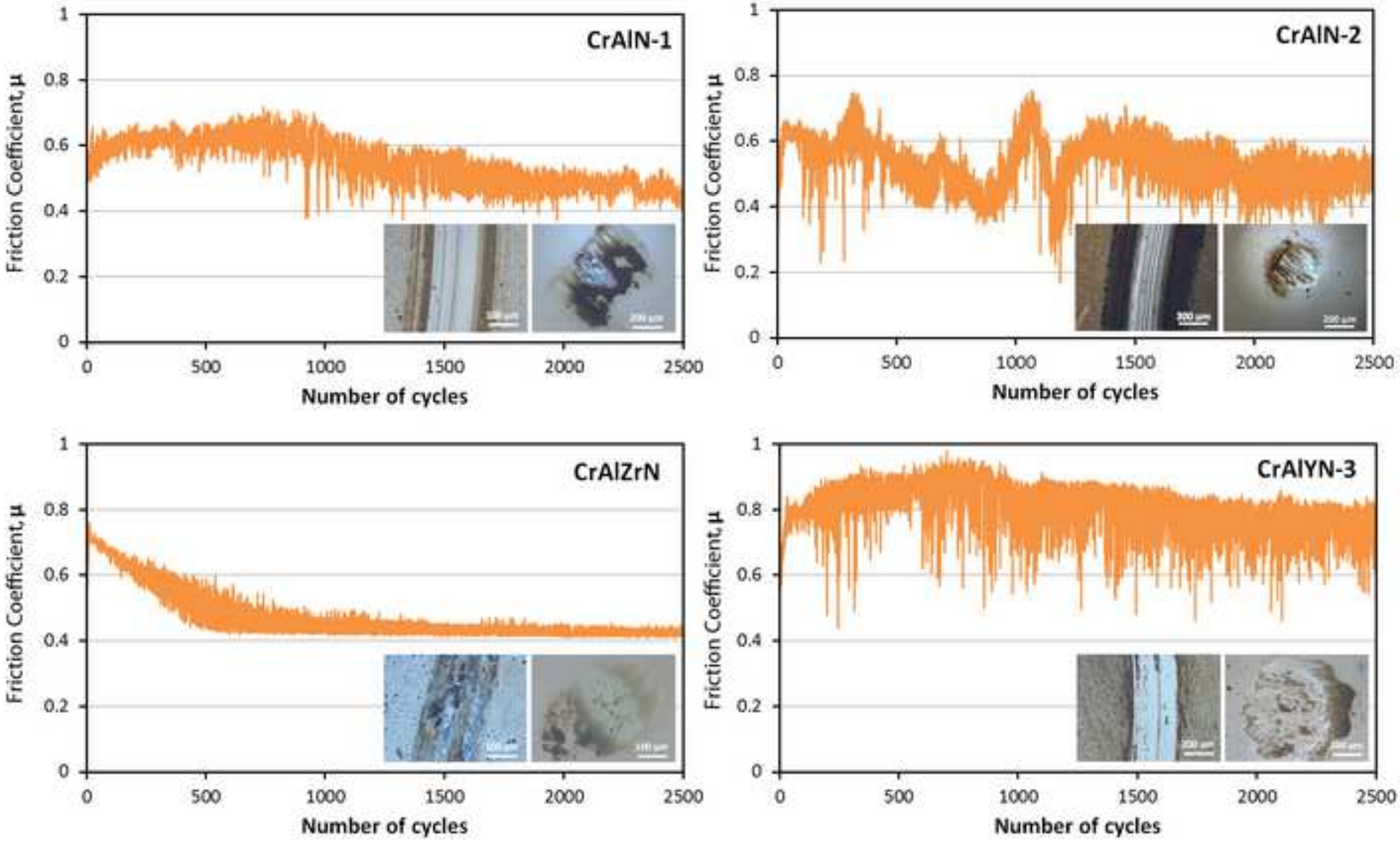

Figure 5

Click here to download high resolution image

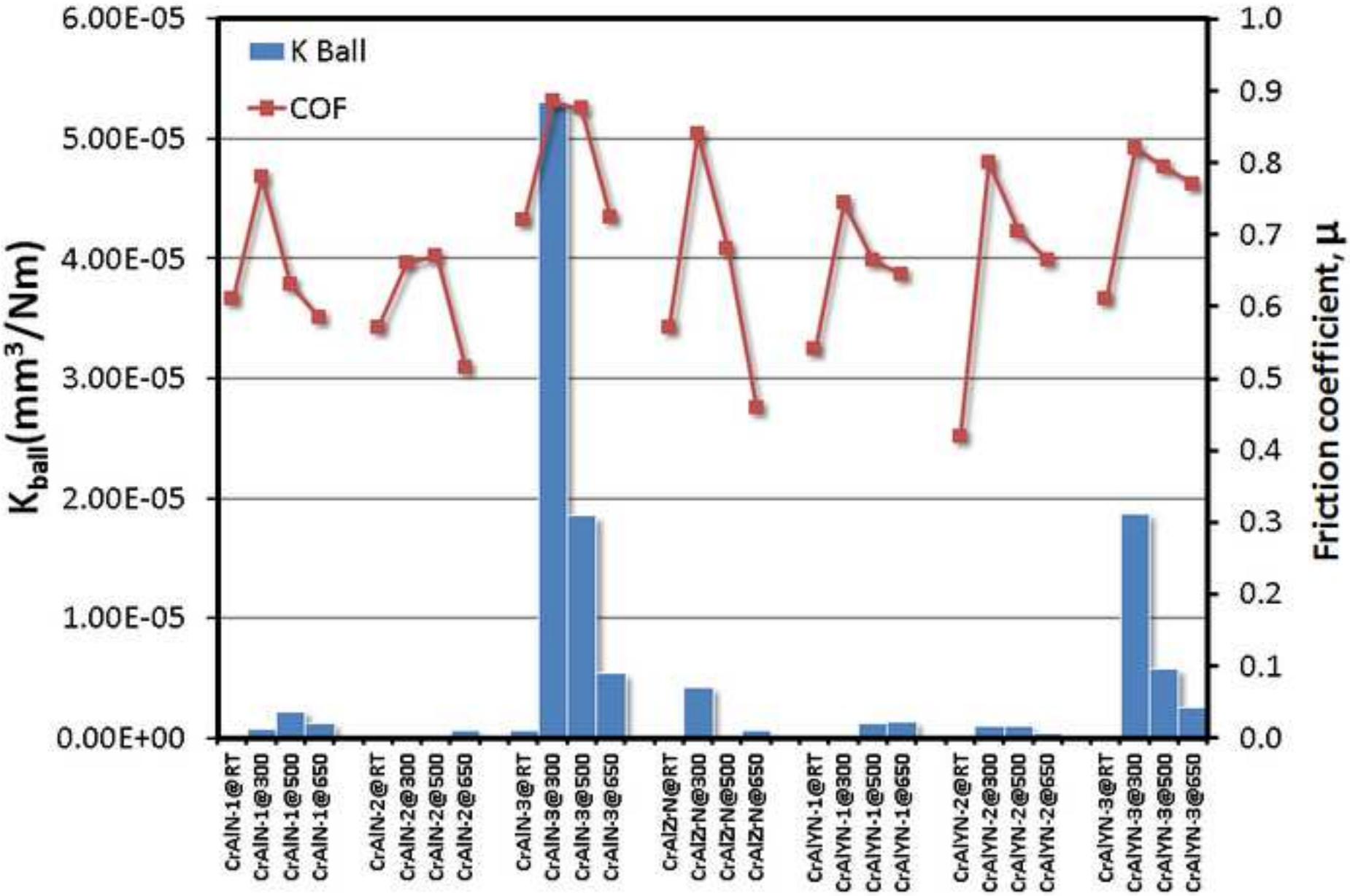

Figure 6

Click here to download high resolution image

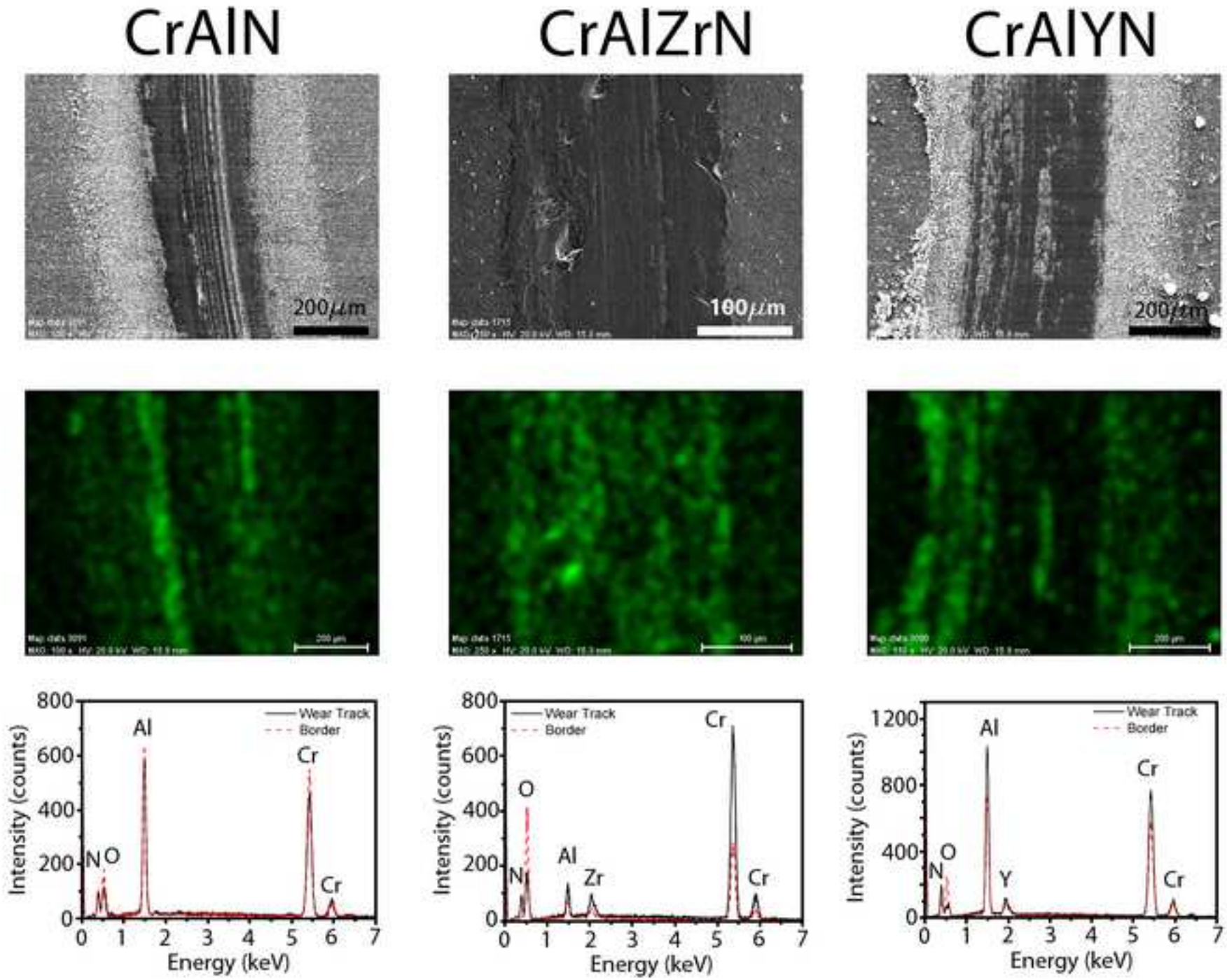

Figure 7

Click here to download high resolution image

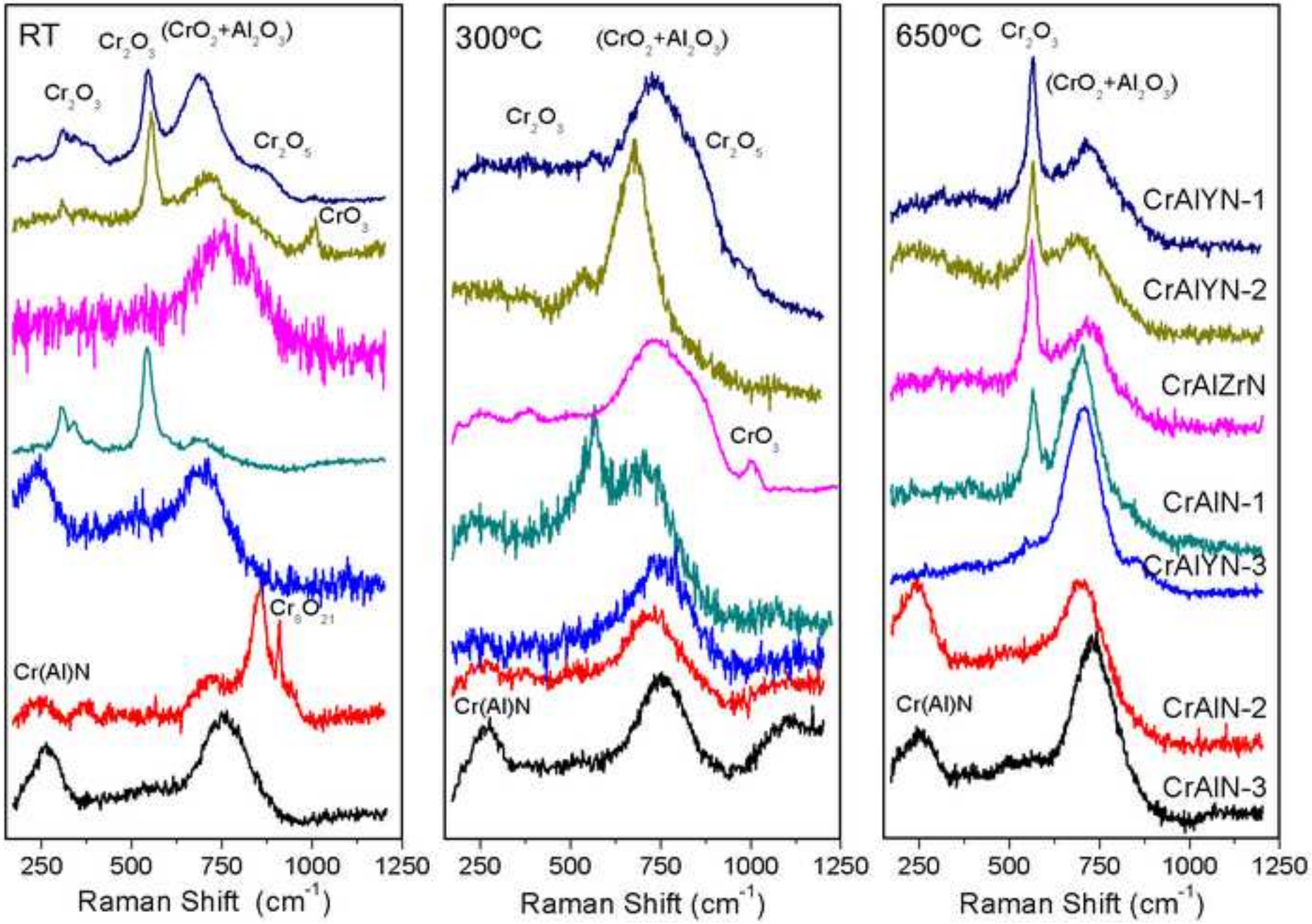

Figure 8
Click here to download high resolution image